

Theoretical Study of Steam Condensation Induced Water Hammer Phenomena in Horizontal Pipelines

Imre Ferenc Barna^{*,1} and Attila Rikárd Imre²

1) *Wigner Research Centre of the Hungarian Academy of Sciences,
1121 Budapest, Konkoly Thege út 29-33, Hungary*

Tel: +36-1-392-2222/3504, Fax: +36-1-395-9151

2) *Energie Research Center of the Hungarian Academy of Sciences,
Konkoly Thege ut 29-33, 1121, Budapest, Hungary*

Abstract

We investigate steam condensation induced water hammer (CIWH) phenomena and present new theoretical results. We use the WAHA3 model based on two-phase flow six first-order partial differential equations that present one dimensional, surface averaged mass, momentum and energy balances. A second order accurate high-resolution shock-capturing numerical scheme was applied with different kind of limiters in the numerical calculations. The applied two-fluid model shows some similarities to Relap5 which is widely used in the nuclear industry to simulate nuclear power plant accidents. This model was validated with different CIWH experiments which were performed in the PMK-2 facility, which is a full-pressure thermo-hydraulic model of the nuclear power plant of VVER-440/312 type in the Energy Research Center of the Hungarian Academy of Sciences in Budapest and in the Rosa facility in Japan. In our recent study we show the first part of a planned large database which will give us the upper and lower flooding mass flow rates for various pipe geometries where CIWH can happen. Such a reliable database would be a great help for future reactor constructions and scheming.

Keywords: steam condensation induced water hammer, two-phase flow

1. Introduction

Safety of nuclear reactors is a fundamental issue. Nuclear and thermo-hydraulic processes in the active zone of modern reactors are well known and well-controlled, explosions are out of question. However, violent unwanted thermo-hydraulic transients in the primer loop may cause serious deformation or pipe breakage. Such an unplanned transient is the CIWM. In thermal loops of atomic reactors or in other pipelines where water steam and cold water can mix, quick and dangerous transients can happen causing pressure surges which mean high financial expenses or even cost human lives. In the following we will present the WAHA3 model [1], which is a complex physical model suitable to simulate various quick transients in single and two-phase flows, such as ideal gas Riemann problem, critical flow of ideal gas in convergent-divergent nozzle, rapid depressurization of hot liquid from horizontal pipes and column separation water hammer or even CIWH. In the last two decades the nuclear industry developed a few complex two-phase flow-codes like RELAP5 [2], TRAC [3] or CATHARE [4] which are feasible to solve safety analysis of nuclear reactors and model complicated two-phase flow transients. The model, WAHA3 has some similarities with RELAP5. This means that the conservation equations are the same but the applied correlations are partially different. The main difference between the above mentioned models and our WAHA3 code is basically the applied numerical scheme; other commercial codes have a ratio of spatial and time resolution $\Delta x/\Delta t$ which describes usual flow velocities. WAHA3, however is capable of capturing shock waves and describe pressure waves which may propagate quicker than the local speed of sound. As a second point WAHA3 has a quick condensation model which is not available for RELAP5 and CATHARE.

2. Experimental Facility

This is a theoretical and numerical study, the used experimental facilities PMK2, and ROSA were mentioned in our former studies where validations were also made[6, 7].

*barna.imre@wigner.mta.hu

3. Numerical Scheme

There are large number of different two-phase flow models with different levels of complexity [8, 9, 10] which are all based on gas dynamics and shock-wave theory. In the following we present the one dimensional six-equation equal-pressure two-fluid model. The density, momentum and energy balance equations for both phases are the following:

$$\frac{\partial A(1-\alpha)\rho_l}{\partial t} + \frac{\partial A(1-\alpha)\rho_l(v_l - w)}{\partial x} = -A\Gamma_g \quad (1)$$

$$\frac{\partial A\alpha\rho_g}{\partial t} + \frac{\partial A\alpha\rho_g(v_g - w)}{\partial x} = A\Gamma_g \quad (2)$$

$$\begin{aligned} \frac{\partial A(1-\alpha)\rho_l v_l}{\partial t} + \frac{\partial A(1-\alpha)\rho_l v_l(v_l - w)}{\partial x} + A(1-\alpha)\frac{\partial p}{\partial x} - A \cdot CVM \\ - Ap_i \frac{\partial \alpha}{\partial x} = AC_i |v_r| v_r - A\Gamma_g v_l + A(1-\alpha)\rho_l \cos(\theta) - AF_{l,wall} \end{aligned} \quad (3)$$

$$\begin{aligned} \frac{\partial A\alpha\rho_g v_g}{\partial t} + \frac{\partial A\alpha\rho_g v_g(v_g - w)}{\partial x} + A\alpha\frac{\partial p}{\partial x} - A \cdot CVM - Ap_i \frac{\partial \alpha}{\partial x} = \\ AC_i |v_r| v_r - A\Gamma_g v_g + A\alpha\rho_g \cos(\theta) - AF_{g,wall} \end{aligned} \quad (4)$$

$$\begin{aligned} \frac{\partial A(1-\alpha)\rho_l e_l}{\partial t} + \frac{\partial A(1-\alpha)\rho_l e_l(v_l - w)}{\partial x} + p\frac{\partial A(1-\alpha)}{\partial t} + \\ \frac{\partial A(1-\alpha)p(v_l - w)}{\partial x} = AQ_{il} - A\Gamma_g(h_l + v_l^2/2) + A(1-\alpha)\rho_l v_l g \cos(\theta) \end{aligned} \quad (5)$$

$$\begin{aligned} \frac{\partial A\alpha\rho_g e_g}{\partial t} + \frac{\partial A\alpha\rho_g e_g(v_g - w)}{\partial x} + p\frac{\partial A\alpha}{\partial t} + \\ \frac{\partial A\alpha p(v_g - w)}{\partial x} = AQ_{ig} - A\Gamma_g(h_g + v_g^2/2) + A\alpha\rho_g v_g g \cos(\theta) \end{aligned} \quad (6)$$

Index l refers to the liquid phase and the index g to the gas phase. Nomenclature and variables are described at the end of the manuscript. Left hand side of the equations contains the terms with temporal and spatial derivatives. Hyperbolicity of the equations is ensured with the virtual mass term CVM and with the interfacial term (terms with p_i). Terms on the right hand

side are terms describing the inter-phase heat, mass (terms with Γ_g) vapor generation rate, volumetric heat fluxes Q_{ij} , momentum transfer (terms with C_i), wall friction $F_{g,wall}$, and gravity terms. Modeling of the inter-phase heat, mass and momentum exchange in two-phase models relies on correlations which are usually flow-regime dependent. The system code RELAP5 has a very sophisticated flow regime map with a high level of complexity. WAHA3 however has the most simple flow map with dispersed and horizontally stratified regimes only. The uncertainties of steady-state correlations in fast transients are very high. A detailed analysis of the source terms can be found elsewhere [5]. Two additional equation of states(eos) are needed to close the system of Eqs. (1-6.) Here the subscript k can have two values l for liquid phase, and g for gas phase

$$\rho_k = \left(\frac{\partial \rho_k}{\partial p} \right)_{u_k} dp + \left(\frac{\partial \rho_k}{\partial u_k} \right)_p du_k \quad (7)$$

Partial derivatives in Eq. 7 are expressed using pressure and specific internal energy as an input. The table of water and steam properties was calculated with a software from UCL [11]. The system of Eqs. (1-6) represents the conservation laws and can be formulated in the following vectorial form

$$\underline{\underline{A}} \frac{\partial \overline{\Psi}}{\partial t} + \underline{\underline{A}} \frac{\partial \overline{\Psi}}{\partial x} = \overline{S} \quad (8)$$

where $\overline{\Psi}$ represents a vector of the non-conservative variables

$\overline{\Psi}(p, \alpha, v_l, v_g, u_l, u_g)$ and $\underline{\underline{A}}, \underline{\underline{B}}$ are 6-times-6 matrices and \overline{S} is the source vector of non-differential terms. These three terms can be obtained from Eq. (1-6) with some algebraic manipulation. In this case the system eigenvalues which represent wave propagation velocities are given by the determinant $\det(\underline{\underline{A}} - \lambda \underline{\underline{B}})$. An improved characteristic upwind discretization method is used to solve the hyperbolic equation system (Eq. 8). The problem is solved with the combination of the first- and second-order accurate discretization scheme by the so-called flux limiters to avoid numerical dissipation and unwanted oscillations which appear in the vicinity of the non-smooth solutions. Exhaustive details about the numerical scheme can be found in the work of [12].

4. Results and Discussion

In our recent study we investigated pipe lines with three different diameters ($D=10, 20, 50$ cm) with three different tube aspect ratio ($L/D=25, 50, 75$) and with three different pressures ($p=10, 20, 40$ bar). These are physically relevant geometries with pressures values which are interesting in various nuclear facilities. Table I presents these system parameters with the minimal and the maximal mass flow rates in between CIWH events happen. For a better transparency these results are presented on Fig 1, 2 and 3 for the different pipe diameters. With this useful representation we can immediately see the dangerous CIWH range between the upper and lower flooding mass flow rates. For completeness we explain additional technical details of our investigations. In all calculations we used the same nodalization in the sense that the actual length of the node is equal to the actual pipe diameter. In all calculations the same Courant-Friedrich-Levy limit was applied with 0.8. As numerical scheme the MINMOD limiter was used. There are only two exceptions at $D=50$, $L/D=50, 75$ $p=20$ bar. The temperature of the cold water was fixed to 293 K. Each presented system (e.g. $D=10$ cm, $L/D=25$, $p=20$ bar minimal mass flow rate) means at least 10 independent calculations with slightly different mass flow parameters. For the maximal flow a calculation takes 20 minutes or even less but for the minimal flow rate one calculation might take 20 hours. To determine if a CIWH event happened we simple checked the pressure-time history closed to the cold water inlet visually. If a sharp peak with a 2 milisecond FWHM can be seen than we are in the dangerous water hammer region. It is worth to note that, our experience shows that there is a very sharp border at both sides of the CIWH regime in this WAHA3 model. Unfortunately, the curves in Figure 1, 2, 3 are not parallel and cross each other which is a confusing problem at this moment. As explanation we think to say that, with additional very time consuming tuning of all the technical parameters (limiter, CFL condition, nodalisation) some of the border points could be slightly modified, but this was not possible till now.

5. Conclusions

We presented the WAHA3 numerical model which is capable to describe supersonic two-phase flow transients in pipe lines. After our former CIWH studies [6, 7], we presented now a database where the minimal and maximal

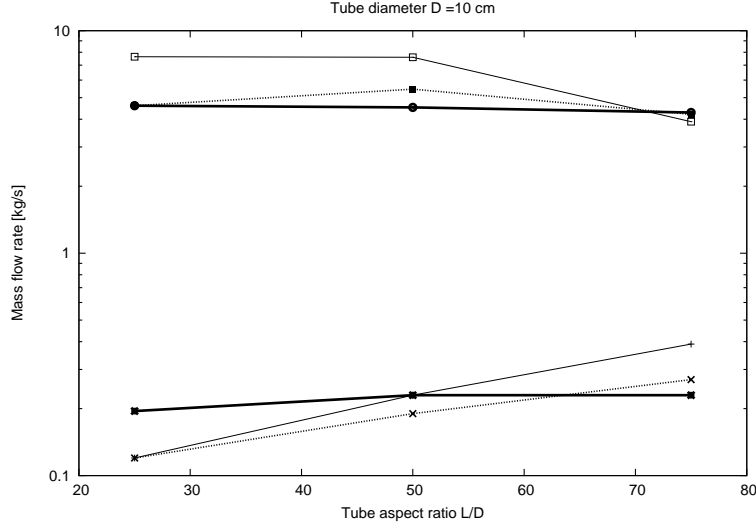


Figure 1: The minimal and maximal mass flow rates for the $D=10$ cm diameter pipelines for $L/D = 25, 50, 75$ tube aspect ratios. The thin solid curve is for $p = 10$ bar, the dashed is for $p = 20$ bar, and the thick solid one is for $p = 40$ bar.

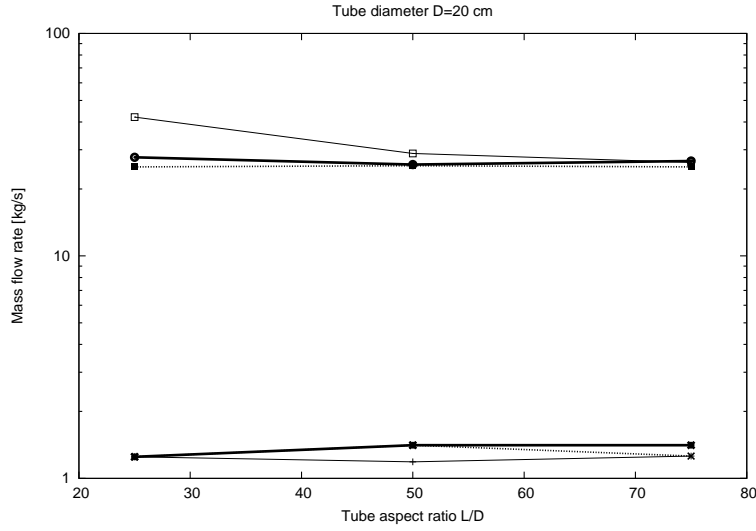


Figure 2: The minimal and maximal mass flow rates for the $D=20$ cm diameter pipelines for $L/D = 25, 50, 75$ tube aspect ratios. The thin solid curve is for $p = 10$ bar, the dashed is for $p = 20$ bar, and the thick solid one is for $p = 40$ bar.

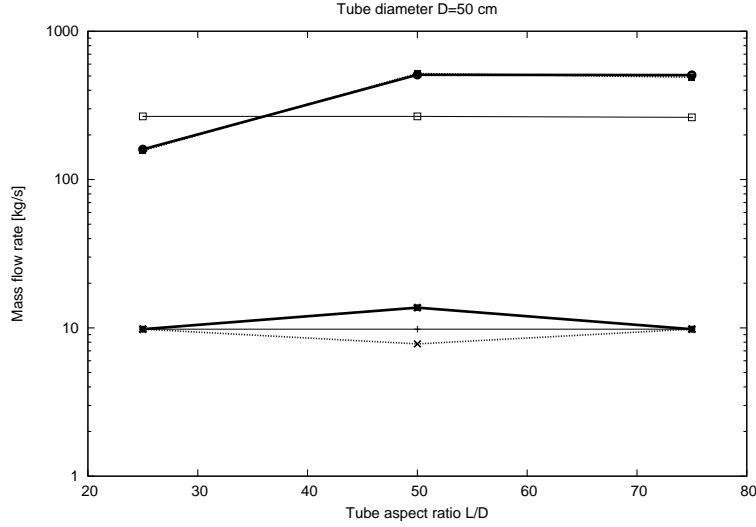


Figure 3: The minimal and maximal mass flow rates for the D=50 cm diameter pipelines for $L/D = 25, 50, 75$ tube aspect ratios. Thin solid curve is for $p = 10$ bar, the dashed curve is for $p = 20$ bar, and the thick solid one is for $p = 40$ bar

mass flow rates can be determined for large number of flow systems. We plan to go further and enhance our database for even larger number of systems.

6. Acknowledgements

We thank Prof. Dr. Iztok Tiselj (Jozef Stefan Institute, Ljubljana, Slovenia) for his fruitful discussions and valuable comments.

References

- [1] I. Tiselj, A. Horvath, G. Cerne, J. Gale, I. Parzer, B. Mavko, M. Giot, J.M. Seynhaeve, B. Kucienska and H. Lemonnier, WAHA3 code manual, Deliverable D10 of the WAHALoads project, March 2004.
- [2] K.E. Carlson, R.A. Riemke, S.Z. Rouhani, R. W. Shumway and W. L. Weaver RELAP5/MOD3.3Beta Code Manual, Vol 1-7, NUREG-CR/5535, EG&G Idaho, Idaho Falls 2003.

- [3] TRAC-PF1/MOD1: An Advanced Best-Estimate Computer Program for Pressurized Water Reactor Thermal-Hydraulic Analysis, NUREG/CR-3858, L.A-10157-MS, 1986.
- [4] D. Bestion and G. Geffraye, The CATHARE code CEA Grenoble Report, DTP/SMTH/LMDS/EM/22001-63, April 2002.
- [5] I. Tiselj and S. Petelin, Modeling of Two-Phase Flow with Second- Order Accurate Scheme, Journal of Comput. Phys., 136 (1997) 503- 521.
- [6] I.F. Barna, A.R. Imre, G. Baranyai and Gy. Ezsol, Experimental and theoretical study of steam condensation induced water hammer phenomena, Nuclear Engineering and Design, 240 (2010) 146.
- [7] I.F. Barna and Gy. Ezsol, Multiple condensation induced water hammer events, experiments and theoretical investigation Kerntechnik, 76 (2011) 231.
- [8] H.B. Stewart and B. Wendroff, Two-Phase flow: Models and Methods, J. Comp. Phys., 56 (1984) 363.
- [9] R. Menikoff. and B. Plohr, The Riemann Problem fluid flow of real materials, Rev. Mod. Phys., 61 (1989) 75.
- [10] M. Ishii and T. Hibiki Thermo-Fluid Dynamics of Two-Phase Flow Springer, 2011, ISBN 978-1-4419-7984-1
- [11] J.M. Seynhaeve, Water properties package, Catholic University of Louvain (1992) Project Built with IAPS from Lester, Gallaher and Kell, McGraw-Hill 1984.
- [12] R. J. LeVeque Numerical Methods for Conservation Laws, Lecture in Mathematics, ETH, Zurich, (1992).

System Parameters	Minimal mass flow rate (kg/s)	Maximal mass flow rate (kg/s)
D = 10 cm		
<i>L/D = 25</i>		
p = 10 bar	0.12	7.64
p = 20 bar	0.12	4.60
p = 40 bar	0.195	4.60
<i>L/D = 50</i>		
p = 10 bar	0.23	7.64
p = 20 bar	0.19	5.46
p = 40 bar	0.23	4.52
<i>L/D = 75</i>		
p = 10 bar	0.39	3.90
p = 20 bar	0.27	4.21
p = 40 bar	0.23	4.29
D = 20 cm		
<i>L/D = 25</i>		
p = 10 bar	1.25	42.08
p = 20 bar	1.25	25.12
p = 40 bar	1.25	27.75
<i>L/D = 50</i>		
p = 10 bar	1.18	28.89
p = 20 bar	1.41	25.43
p = 40 bar	1.41	25.75
<i>L/D = 75</i>		
p = 10 bar	1.26	26.38
p = 20 bar	1.26	25.12
p = 40 bar	1.41	26.70
D = 50 cm		
<i>L/D = 25</i>		
p = 10 bar	9.8	266.5
p = 20 bar	9.8	156.8
p = 40 bar	9.8	160.0
<i>L/D = 50</i>		
p = 10 bar	9.8	266.55
p = 20 bar	7.8	519.4
p = 40 bar	13.7	509.0
<i>L/D = 75</i>		
p = 10 bar	9.8	262.66
p = 20 bar	9.8 ¹⁰	490.0
p = 40 bar	9.8	505.6

Table I. The minimal and maximal mass flow rates for the investigated systems.

7. Nomenclature

A	pipe cross section (m^2)
C_i	internal friction coefficient (kg/m)
CVM	virtual mass term (N/m^3)
e_i	specific total energy [$e = u + v^2/2$] (J/kg)
$F_{g,wall}$	wall friction per unit volume (N/m)
g	gravitational acceleration (m/s^2)
h_i	specific enthalpy [$h = u + p/\rho$] (J/kg)
p	Pressure (Pa)
p_i	interfacial pressure $p_i = p\alpha(1 - \alpha)$ (Pa)
Q_{ij}	interf.-liq./gas heat transf. per vol. rate (W/m^3)
t	time (s)
u_i	specific internal energy (J/kg)
v_i	velocity (m/s)
v_r	relative velocity ($v_r = v_g - v_f$) (m/s)
w	pipe velocity in flow direction (m/s)
x	spatial coordinate (m)
Greek letters	
α	vapour void fraction
Γ_g	vapour generation rate (kg/m^3)
ρ_i	density (kg/m^3)
θ	pipe inclination (<i>degree</i>)
Subscripts	
l	liquid phase
g	gas phase